

Published in final edited form as:

Biomacromolecules. 2010 December 13; 11(12): 3592–3599. doi:10.1021/bm101054q.

Quantifying Osteogenic Cell Degradation of Silk Biomaterials

Sejuti Sengupta, MS¹, Sang-Hyug Park, PhD¹, Gil Eun Seok, PhD¹, Atur Patel, BS¹, Keiji Numata, PhD¹, Chia-Li Lu, MS¹, and David L. Kaplan, PhD.^{1,*}

¹ Biomedical Engineering, School of Engineering, Tufts University, 4 Colby St. Medford 02155, MA. USA

Abstract

The degradation of silk protein films by human mesenchymal stem cells (hMSCs), osteoblasts and osteoclasts, cells involved in osteogenic functions in normal and diseased bone, was assessed in vitro. The involvement of specific matrix metalloproteinases (MMPs) and integrin signaling in the degradation process was determined. Scanning electron microscopy (SEM) and atomic force microscopy (AFM) were used to quantitatively compare degradation by the different cell types using surface patterned silk films. Osteoblasts and osteoclasts demonstrated significant degradation of the silk films in vitro in comparison to the hMSCs and the film controls without cells. The osteoclasts degraded the silk films the most and also generated the highest level of MMPs 1 and 2. The osteoblasts upregulated integrins $\alpha 5$ and $\beta 1$ while the osteoclasts upregulated integrins $\alpha 2$ and $\beta 1$. There was significant contrast in responses on the silk matrices between osteogenic cells vs undifferentiated hMSCs to illustrate in vitro the role of cell type on matrix remodeling. These are important issues in matching biomaterial matrix features and studies in vitro to remodeling in vivo, in both normal and disease tissue systems. Cell populations and niche factors impact tissue regeneration, wound healing and physiological state and the ability to better understand the role of different cell types is critical to overall regenerative outcomes.

Keywords

Degradation; Silk; Bone; regeneration; Osteoblasts; Osteoclasts; hMSCs; MMPs; Integrins

Introduction

One goal of tissue engineering is to regenerate lost or damaged tissue by supporting the growth or differentiation of desired cell types on biomaterial substrates often designed to mimic the ECM. In addition, opportunities to generate functional human tissues in vitro to represent in vivo physiological states, native or disease, is a direction of interest with tissue engineered systems. The dynamic relationship between cells and biomaterials must be understood for tissue engineering strategies to be relevant for both goals. Native ECM is continuously remodeled in vivo by synchronous proteolytic degradation and reassembly by cells in a complex orchestrated set of events [1]. Similarly, useful bone regenerative matrices should direct cells to adhere, migrate and degrade the starting biomaterial in order to activate downstream signaling and regenerate new bone tissue at the repair site [2]. The rate at which the starting biomaterial matrix degrades and is fully replaced by native ECM dictates the success of the tissue engineering strategy.

Different matrix features are known to influence the rate and extent of tissue remodeling [3]. For instance, the degradation kinetics of collagen scaffolds and alginate gels affected bone

*Corresponding author: David L. Kaplan, PhD, David.Kaplan@tufts.edu, Telephone: 617-627-3251, Fax: 617-627-3231.

tissue formation [4]. Increased rates of degradation of polyethylene glycol (PEG) hydrogels increased ECM distribution by chondrocytes in vitro [5]. Silk has been used as a biomaterial for bone tissue engineering [6], and we have previously reported that bone regeneration rate and morphology can be altered by matching silk scaffold design features to rates of degradability in vitro [7,8]. The susceptibility of silk to proteolytic degradation by enzymes like protease XIV, α -chymotrypsin and collagenase 1a, has been investigated [9]. However, there is a need to better understand the interrelationships of matrix design, matrix degradation and cell type and interactions related to tissue regeneration. Consequently, in the present study, the degradation of silk matrices by osteogenic cells in vitro was studied.

Cell adhesion to native ECM is mediated by integrins, which bind to specific amino acid sequences such as arginine–glycine–aspartic acid (RGD) [10]. As the cells attach to the matrix, they secrete matrix metalloproteinases (MMPs) which act on specific MMP cleavage sites. The subsequent degradation by MMPs enables further cell ingrowth into matrices to carry out bone remodeling [11]. This process involving integrins and MMPs is integral to osteogenic differentiation. MMP-mediated degradation is involved in the release of bone morphogenic protein-2 (BMP-2), which signals osteoblast precursor cells to differentiate and secrete bone matrix [2]. MMPs have been implicated in the controlled degradation of collagen and other matrix substrates during bone regeneration [11]. However, the involvement of MMPs in silk degradation during bone regeneration has not been documented. The collagenase members of the matrix metalloproteinase (MMP) family of enzymes which target collagen type I, modulate osteoblastic differentiation by degrading collagen [12]. Since collagen is deposited during osteoblastic differentiation of hMSCs on silk protein scaffolds [13], the role of MMPs (or collagenases) during osteogenic differentiation on silk films was determined in the present study.

MMPs are endopeptidases involved in the degradation of ECM components and play an important role in tissue remodeling and morphogenesis [14]. MMP-1 (collagenase-1) and MMP-13 (collagenase-3) are key enzymes responsible for degrading type I collagen and regulating osteoblastic differentiation [11]. In addition, MMP9 (gelatinase B) and MMP13 play critical roles in regulating endochondral ossification, a bone formation process which relies on ECM degradation [15]. Dysregulation of MMP2 and MMP13 caused osteolytic diseases, decreased bone mineralization and resulted in defective growth of osteoblasts and osteoclasts [11,15]. MMP-2 (gelatinase A) is a type IV collagenase, responsible for the formation of osteocytic canalicular networks which are important for bone remodeling and mineralization [16]. Matrix-integrin signaling is another important factor directly influencing osteoblastic differentiation. Type I collagen-induced osteoblastic differentiation of bone-marrow cells is mediated by collagen- α 2 β 1 integrin interactions, with osteoblast differentiation inhibited by disrupting α 2-integrin- and/or β 1-integrin-type I collagen interactions [17]. Binding of α 5 β 1 to fibronectin is critical to many cellular processes, including osteoblast and myoblast differentiation [11]. In light of these previous findings, expression levels of MMP1, MMP2, MMP9, MMP13, ITGA2 (integrin α 2), ITGA5 (integrin α 5) and ITGB1 (integrin β 1) were assessed in the present study.

A group of secreted proteins known as the tissue inhibitors of metalloproteinases (TIMPs) perform an important physiological regulatory mechanism to block the proteolytic activity of MMPs. TIMPs have the ability to attenuate ECM degradation and indirectly influence ECM-dependent signal transduction by inhibiting MMP activity [18]. Human osteoblasts constitutively express TIMP-1 [19], which binds to most MMPs, including MMP1, MMP2, MMP9, MMP13, to form non-covalent complexes and, thereby, block access of substrates to the catalytic site of MMPs [14,19]. Therefore, TIMP-1 secretion by the cells was assessed to confirm MMP activity. In order to account for other post-transcriptional modes of MMP regulation, the secretion of MMPs by the osteogenic cells was also assessed.

The degradation of silk biomaterials with accompanying cell infiltration and the generation of new ECM is critical for the integration of in vitro grown bone in the body. Therefore, the goal of the present in vitro study was to assess the degradation of silk films by osteogenic cells and understand some of the underlying mechanisms. In particular, we were interested in using this biomaterial matrix as a simplified platform to compare degradation roles by different cell types, all of which are involved in osteogenic processes, including normal and disease bone states. The degradation ability of human mesenchymal stem cells (hMSCs), human osteoblasts and human osteoclasts was therefore assessed within the context of degradation, MMP functions and integrin signaling. The osteoblasts were differentiated from the human bone-marrow derived hMSCs [10] and the osteoclasts were differentiated from human monocytic precursor cells [20,21].

Experimental Section

Patterned silk film fabrication

Cocoons of *Bombyx mori* were boiled for 30 min in an aqueous solution of 0.02 M Na₂CO₃, and then rinsed thoroughly with distilled water to eliminate the glue-like sericin proteins. The extracted silk fibroin was dissolved in 9.3 M LiBr solution at 60°C for 4 h, yielding a 20 w/v% solution. This solution was dialyzed in distilled water using a Slide-a-Lyzer dialysis cassette (MWCO 3,500, Pierce) for 2 days [13]. The final concentration of silk fibroin aqueous solution was 8% w/v. Patterned polydimethylsiloxane (PDMS) (GE Plastics) substrates of 2–3 mm thickness were prepared by casting on 1,200 lines/mm (blaze angle 17°/27") diffraction grating (Edmund Optics, Inc.) surfaces. PDMS rounds were punched with 11 mm diameters. The PDMS substrates were placed cast side up, and prepared for silk casting by a 70% ethanol wash with three DI water washes. A 62 µL aliquot of 8% silk solution was cast on the grooved PDMS substrates to generate a 50 µm thick film [22]. The films were covered with a venting lid and allowed to dry overnight. Once dried, a water-annealing processing was performed by placing the silk film within a water-filled dessicator at 24 mm Hg vacuum for a 5 h period. The silk films were removed from their PDMS substrates and placed onto 24-well non-tissue culture plates, with the patterned surface on top. The films were sterilized with 70% ethanol and washed three times in ultrapure dH₂O. Finally, the films were pre-wetted in media for cell seeding.

Cell seeding and cultivation

hMSC isolation from total bone marrow was carried out as previously reported [23]. These cells were then expanded in hMSC growth medium (DMEM supplemented with 10% FBS, 0.1 mM nonessential amino acids, 1 ng/ml bFGF in the presence of 100 U/ml penicillin, 100 µg/ml streptomycin, and 0.25 µg/ml fungizone) at 37°C in a 5% CO₂ incubator. A human monocyte cell line originally isolated from the peripheral blood of an acute leukemia patient, THP-1 (American Type Culture Collection (ATCC) TIB-202™, VA) was expanded in growth media (RPMI-1640 supplemented with 10% FBS, 0.1 mM nonessential amino acids, 0.05 mM 2-mercaptoethanol in the presence of 100 U/ml penicillin, 100 µg/ml streptomycin, and 0.25 µg/ml fungizone) at 37°C in a 5% CO₂ incubator. The monocytes were then treated with 200 ng/ml of phorbol-12-myristate-13-acetate (PMA) (Sigma, MO) to induce the maturation into macrophages [20].

P2 hMSCs and THP-1 cell-derived macrophages were detached from the T-flasks by 0.25% trypsin (Sigma, MO) and seeded onto their respective prewetted patterned silk films at a density of 500,000 cells per film at 37°C in a 5% CO₂ incubator. Two hours after cell seeding the films were immersed in 2 ml of their respective media (Table 1). Group 1 consisted of hMSCs maintained in hMSC growth media while group 2 consisted of hMSCs maintained in osteoblastic differentiation media (hMSC growth media supplemented with

the differentiation factors - 50 µg/ml ascorbic acid-2-phosphate, 100 nM dexamethasone and 10 mM β-glycerolphosphate) [13]. Group 3 consisted of macrophages maintained in osteoclast differentiation media (RPMI-1640 supplemented with 10% FBS, 100 U/ml penicillin, 100 µg/ml streptomycin, 0.25 µg/ml fungizone, 0.1 mM nonessential amino acids, 0.05 mM 2-mercaptoethanol in the presence of 200 ng/ml of PMA and 25 ng/ml receptor activator of NF-κB ligand (RANKL)). Addition of RANKL induces differentiation and activation of osteoclasts from precursor macrophage cells [21]. Group 4 was the negative control with no cells maintained in DMEM supplemented with 10% FBS. Half of the media was replaced every 3 days. Complete media change was carried out every two weeks when the films were transferred to a new plate.

Picogreen analysis

At week 4, 1 ml of 0.25% trypsin was added to each group (N=3 samples per group) and incubated at 37°C for 10 minutes. The samples were then washed with 1 ml of the respective media to collect 2 ml of cell suspension. One ml of the resulting cell suspension was subjected to the Picogreen assay (Molecular Probes, Eugene, OR) for DNA quantification according to the manufacturer's instructions. Samples were measured fluorometrically at an excitation wavelength of 480 nm and an emission wavelength of 528 nm.

Real time PCR

The remaining 1 ml of the cell suspension was stored with 1 ml of Trizol at -80°C. The samples were then subjected to real time PCR. Two hundred µl of chloroform was added to the supernatant following centrifugation at 12,000 g for 10 min, and incubated for 5 min at room temperature. After centrifugation at 12,000 g for 15 min, the upper aqueous phase was transferred to a new Eppendorf tube. One volume of 70% ethanol (v/v) was added and applied to an RNeasy mini spin column (Qiagen, Hilden, Germany). The RNA was washed and eluted according to the manufacturer's protocol. The RNA samples were reverse transcribed into cDNA using oligo (dT)-selection according to the manufacturer's protocol using a High Capacity cDNA Archive Kit (Applied Biosystems, Foster City, CA). Transcript levels of MMP1, MMP2, MMP9, MMP13, ITGA2, ITGA5, ITGB1 were quantified using the M3000 Real Time PCR system (Stratagene, CA). PCR reaction conditions were 2 min at 50°C, 10 min at 95°C, and then 50 cycles at 95°C for 15 s, and 1 min at 60°C. The expression data were normalized to the expression of the housekeeping gene, glyceraldehyde-3-phosphate-dehydrogenase (GAPDH). Primer sequences for the human GAPDH gene were: forward primer 5'-ATGGGGAAGGTGAAGGTCG-3', reverse primer 5'-TAAAAGCCCTGGTGACC-3' and probe 5'-CGC CCAATACGACCAAATCCG TTG AC-3'. Primers and probes for MMP1, MMP2, MMP9, MMP13, ITGA2, ITGA5, ITGB1 were purchased from Applied Biosciences (FosterCity, CA) Assays-on-Demand™ Gene Expression kits (MMP1, Product # Hs00899660_g1; MMP2, Product # Hs01548724_m1; MMP9, Product # Hs00957554_g1; MMP13, Product # Hs00942589_m1; ITGA2, Product # Hs00985378_m1; ITGA5, Product # Hs01565675_m1; ITGB1, Product # Hs01127543_m1). Finally, the transcript levels of different groups were expressed in terms of fold increase relative to the negative control group (group 4).

Silk film analysis

After treatment with 0.25% trypsin (1 ml/well) for 10 minutes at week 4, the remaining cells were removed from the silk films by 1 hour cold shock at -20°C followed by incubation in cold water at 4°C overnight. The silk films were then cut in two halves for SEM and AFM analysis.

Scanning electron microscopy (SEM)

One half of each silk film (N=3 samples per group) was dried and gold coated for 1.5 minutes and observed under SEM (Zeiss, FESEM Supra55VP, Germany) for the presence of degradation pits. The dimensions of the degradation pits caused by the actively degrading cell types were compared by measuring the length and width of the irregular pits across diametrically opposite ends of the pit. The measurements were repeated at ten degradation pits on each film. In addition, the number of degradation pits was compared by quantifying the number of pits in the SEM images. The quantification was done on 3 different points on each of the three replicates.

Atomic force microscopy (AFM)

On the basis of SEM findings, the other half of each silk film was assessed by AFM Dimension V (Veeco Instruments Inc, Plainview, NY) to evaluate the degradation pits. AFM observations were performed in air at room temperature using a 200–250 μm long silicon cantilever with a spring constant of 2.8 N/m in soft tapping mode AFM. Calibration of the cantilever tip-convolution effect was carried out by previously reported methods [24]. The widths and depths of ten degradation pits of each film were measured by means of AFM.

ELISA analysis

At week 4, the media from (N=3 samples per group) each group was stored at -20°C to confirm the secretion of specific MMPs and integrins by ELISA. ELISAs for MMP-1, MMP-2 and TIMP-1 were performed using commercial kits (R&D Systems, MN) following the manufacturer's instructions. Protein concentrations (ng/ml) were determined by standard curves and expressed in terms of fold increase relative to the negative control (group 4).

Statistical analysis

All values are represented as mean \pm Standard deviation. Statistical differences was determined by Student's t test. Statistical significance was assigned as * denoting $p < 0.05$.

Results and Discussion

A schematic representation of the procedures is shown in Figure 1 and the study groups are listed in Table 1.

DNA quantification

Picogreen analysis confirmed the presence of cells in all groups other than the negative control (group 4) at week 4 (Figure 2). There was no significant difference in the DNA content between the different study groups.

Silk film degradation

In a recent study comparing degradable biomaterial films of chitosan, poly L-lactic acid (PLLA) and silk fibroin, silk fibroin was reported to be a suitable biomaterial to support the proliferation and differentiation of a coculture of murine osteoblasts and osteoclasts [25]. The topography of the fibroin film became progressively rougher with time in culture, indicating silk degradation by the osteoclasts [25]. In the present study we sought to evaluate the role of human cells involved in bone remodeling, specifically osteoblasts, osteoclasts and hMSCs, using silk films as substrates. Further, we sought to quantify the process and related these findings to specific MMPs and integrins. Using a well defined silk protein biomaterial surface with surface patterns to facilitate both cell interactions and improve quantitation of surface pitting as a reflection of the film degradation, osteogenic cells, osteoblasts and osteoclasts, actively degraded the films (Figures 3–4).

SEM images show that groups 2 (osteoblasts) and 3 (osteoclasts) generated more degradation pits across the film surfaces (Figures 3c–3f), whereas the hMSCs generated pits with smaller dimensions and there were fewer pits (Figure 3b). In contrast, the negative controls (group 4) showed uniform patterned film surfaces without observable degradation pits (Figures 3a). The number of pits caused by the actively degrading groups 2 (osteoblasts) and 3 (osteoclasts) was quantified from the SEM images. Group 3 (osteoclasts) generated a significantly larger number of pits, when compared to group 2 (osteoblasts) (Table 2). It should be noted that the osteoclasts generated significantly larger pits in certain areas, thereby limiting the number of pits observed in that area. This is accounted by the larger standard deviation in group 3 (Table 2). AFM was also used to quantify the dimensions of the degradation pits (Figure 4). AFM images of a $100 \times 100 \mu\text{m}^2$ section confirmed that groups 2 (osteoblasts) and 3 (osteoclasts) had degradation pits scattered across the surface, a feature absent from group 4 (negative controls) (Figures 4a–c). AFM images of $10 \times 10 \mu\text{m}^2$ sections were taken to compare the widths and depths of degradation pits ($n=10$) in groups 2 (osteoblasts) and 3 (osteoclasts) (Figures 4d–f). From the SEM and AFM images, group 3 (osteoclasts) showed larger and more frequent degradation pits when compared to group 2 (osteoblasts) (Figures 3–4), with a significant difference in length, width and depth of the pits generated by group 3 (osteoclasts), relative to that of group 2 (osteoblasts) (Table 2). The minor differences in pit dimensions between the AFM and SEM images of the same group is accounted for by the larger scanning area for the SEM, enabling the measurement of more widely spaced degradation pits.

During bone remodeling *in vivo*, osteoclasts are specialized cells that perform the function of matrix resorption, whereas osteoblasts promote matrix deposition [26]. Thus, the greater degradation of silk films caused by osteoclasts in this *in vitro* study is in agreement with the *in vivo* bone resorptive ability of this cell type. In addition, hMSCs differentiated into osteoblasts degraded the silk films more actively than undifferentiated hMSCs.

Gene expression and secretion of MMPs and integrins

Prior study using collagen gels as a model system showed that the combined influence of the ECM-degrading function of MMPs and the forces transmitted by integrin $\alpha_2\beta_1$ resulted in enhanced contraction of the gels [27]. These data suggested that MMPs and integrins, in synergy, are useful targets for controlling rates of tissue remodeling [27]. Building on this previous finding, the present study with hMSCs and osteogenic cells illustrated the different rates of bone remodeling orchestrated by differential MMP and integrin activity for each cell type.

Transcript levels of the relevant MMP- and integrin-specific genes at week 4 for each group, expressed in fold increase with respect to the negative control (group 4), are shown in Figure 5. These cell types expressed detectable levels only of MMP1 and MMP2, but not MMP9 and MMP13. The osteoclasts (group 3) showed a significant increase in expression levels of MMP1 and MMP2 compared to all other groups. The hMSCs (group 1) and osteoblasts (group 2) expressed detectable levels of ITGA5 and ITGB1, and the osteoclasts (group 3) expressed detectable levels of ITGA2 and ITGB1. Moreover, the osteoblasts (group 2) expressed significantly higher levels of ITGA5 and ITGB1 than the undifferentiated hMSCs (group 1). The level of MMP1, MMP2 and TIMP-1 proteins secreted into the media ($N=3$ samples per group) expressed in terms of fold increase with respect to the negative control (group 4) is shown in Figure 6. The osteoclasts (group 3) secreted significantly higher levels of MMP1 and MMP2 and significantly lower level of the MMP inhibitor TIMP-1 as compared to all other groups. The hMSCs (group 1) secreted MMP1 and MMP2 levels comparable to the osteoblasts (group 2), but significantly higher levels of TIMP-1 than the osteoblasts (group 2). This is consistent with a recent study showing TIMP-1 secretion by hMSCs which inhibits the activity of exogenous MMP2 and MMP9 secreted by the cells

[28]. While the osteogenic cells (osteoblasts and osteoclasts) in this study interacted with the silk matrix leading to the upregulation of MMPs and integrins, the hMSCs (group 1) did not degrade the silk films significantly and also expressed and secreted significantly lower levels of MMP1 and MMP2 than the osteoclasts (group 3). The significant increase in MMP1 and MMP2 expression in osteoclasts, combined with their high degradation capability in comparison to all other groups, suggests the *in vitro* assay utilized here provides a suitable mimic for the *in vivo* scenario, based on what is known about the respective roles of these cell groups in matrix/bone remodeling. This provides a suitable starting point to move into 3D comparisons, where analytical tracking is more difficult than in the 2D system presented here. Further refinements of the system can include premineralization of the matrices to reflect bone tissue features as part of these systems, with the opportunity to learn how changes in cocultured populations of the cell types used here impact remodeling rates *in vitro*, as predictors of outcomes *in vivo*. All of these directions build off of the baseline insight provided in the present study, wherein quantitative degradation was assessed along with key enzymes and cell membrane receptors, to provide sites for tracking changes in future related studies.

Although the hMSCs (group 1) expressed lower levels of ITGA5 and ITGB1, these integrins were significantly upregulated in the osteoblast group (group 2) (Figure 5), indicating their role in osteoblastic differentiation or functions. Previous reports using a collagen I gel suggested the involvement of ITGA2 and ITGB1 in osteoblast differentiation [17]. However, we did not identify detectable transcript levels of ITGA2 by the osteoblasts (group 2) differentiated *in vitro* on silk films in the present study. This finding can be explained by the presence of distinct adhesion sites on silk. The binding site of integrin ITGA2 on collagen type I, the major ECM protein, is the amino acid sequence GFP*GERGVEGPP*GPA (where P* represents hydroxyproline). The GER sequence was identified as the essential recognition site for ITGA2 to bind collagen type I, since altering/deleting one of amino acid residues in this sequence inhibited ITGA2 binding [29]. Since silk fibroin does not contain the GER sequence [30], affinity with integrin ITGA2 was not found in the present *in vitro* study. In contrast, the primary binding site at which integrin ITGA5 interacts with fibronectin is the amino acid sequence RGD [31]. To bind with integrin ITGA5, the protein is required to have either the binding sequence RGD or a sequence similar to RGD [32]. Although sparse in occurrence, silk fibroin protein contains sequences RGY and RGV [30], which might be one explanation for the binding of ITGA5 to silk fibroin film in the present findings.

An understanding of the specific interactions between the structural features of silk matrices and cellular responses remains to be elucidated; however, the system described here offers a suitable starting point for such inquiry. The surface chemistry of biomaterials, including silk, is an important determinant of MMP cleavage and integrin binding, resulting in the enhancement of cell responses, including cell adhesion and activation of biochemical pathways regulating cellular proliferation, differentiation, and survival [33]. For instance, degradation studies with MMP 1 and MMP 2 and silk fibroin, in the form of porous sheets and films, indicated that MMP1 targeted specific cleavage sites bearing amino acid combinations of -Xaa-Gly [34]. MMP 2 recognized peptide sequences of -Gly-Ile-, -Gly-Val-, -Gly-Gln-, -Gly-Phe-, -Gly-Asn-, and -Gly-Ser [35]. Labeling the cell-specific integrins expressed involved in the remodeling process at the silk film surface will help to pinpoint adhesion sequences on silk which mediate integrin binding.

The role of MMPs and integrins in cell-matrix interaction is especially important in the context of disease conditions. Abnormalities in cellular MMP expression and ECM remodeling often impairs osteogenic capacity leading to diseases like dwarfism, osteopenia, osteoarthritis and skeletal metastasis [1,36]. Malignant cells acquire invasive capabilities by

releasing MMPs to degrade the basement membrane of blood vessels and form a secondary metastatic colony. Also, binding of $\alpha 2\beta 1$ integrin to collagen I increased the colonization of metastatic prostate cancer cells in bone [37]. Thus, the MMP and integrin expression results from the present study could be useful as a baseline to detect abnormally high/low level of these MMPs and integrins in disease conditions using in vitro silk based disease models, like breast cancer metastasis [38] and autosomal dominant polycystic kidney disorder [39].

An important challenge is to link in vitro understanding of functions of MMPs to in vivo scenarios. The identification of MMPs and integrins expressed by bone cells differentiated on silk films provides a starting point towards elucidating signaling pathways activated by the interaction between osteogenic cells and the silk substrate. MMP-mediated changes to the collagenous matrix might alter collagen-integrin interactions or the activation/release of matrix bound growth factors [11]. In native tissue, clustering of integrin molecules on RGD sequences of the matrix is known to phosphorylate focal adhesion kinase (FAK) and reorganize the actin cytoskeleton, which in turn, upregulates/downregulates cellular proliferation and differentiation pathways. The differences in surface chemistry of different biomaterials modulate focal adhesion composition and subsequent signaling, thus regulating osteoblast differentiation and mineralization [40]. Investigations of possible signaling pathways activated by the MMPs and integrins expressed by osteogenic cells on silk fibroin can yield useful information. For example, integrins $\alpha 5$ - and $\beta 1$ -mediated binding of hMSCs to silk films could activate MAPK/ERK pathways (Figure 7), which, in turn, can promote differentiation into osteoblasts [41]. A related study conducted with polyethylene glycol (PEG) hydrogels introduced a peptide sequence incorporating a MMP13 cleavage site and fibronectin binding RGD site, and initiated extensive survival and chondrogenic differentiation of hMSCs [42]. The MMP13 secreted by the hMSCs cleaved the peptide sequences mimicking native differentiation cell-signaling cascades involved in chondrogenic differentiation [42]. A similar silk-based system exploiting cellular remodeling for temporal delivery of ECM cues will enable the design of a niche for osteogenic differentiation, building off of the results of the present study.

Conclusions

Osteogenic cells, osteoblasts and osteoclasts, actively degraded silk fibroin protein in vitro, a biomaterial widely used in bone tissue engineering. The identification of MMP and integrin responses by these cells confirmed the respective contributions to the degradation process. The osteoclasts caused more and larger degradation pits than osteoblasts or hMSCs, and also secreted higher levels of MMP1 and MMP2. Further studies based on the system utilized in the present study will help to identify adhesion sequences on silk and elucidate signaling mechanisms which promote osteoblast and osteoclast differentiation on silk-based biomaterials. These insights will provide useful comparisons to other degradable biomaterials for future designs to optimize remodeling of such matrices to match repair-specific needs.

Acknowledgments

The authors thank Carmen Preda for her technical contributions. This work was supported by NIH P41 Tissue Engineering Resource Center (EB002520) and the NIH (EB003210 and DE017207).

References

1. Daley WP, Peters SB, Larsen M. Extracellular matrix dynamics in development and regenerative medicine. *J Cell Sci.* 2008; 121:255–264. [PubMed: 18216330]
2. Wozney JM, Li RH. Engineering what comes naturally. *Nat Biotech.* 2003; 21:506–508.

3. Abraham LC, Dice JF, Finn PF, Mesires NT, Lee K, Kaplan DL. Extracellular matrix remodeling—Methods to quantify cell–matrix interactions. *Biomaterials*. 2007; 28:151–161. [PubMed: 16893566]
4. Alsberg E, Kong HJ, Hirano Y, Smith MK, Albeiruti A, Mooney DJ. Regulating bone formation via controlled scaffold degradation. *J Dent Res*. 2003; 82:903–8. [PubMed: 14578503]
5. Bryant SJ, Anseth KS. Hydrogel properties influence ECM production by chondrocytes photoencapsulated in poly(ethylene glycol) hydrogels. *J Biomed Mater Res*. 2002; 59:63–72. [PubMed: 11745538]
6. Sofia S, McCarthy MB, Gronowicz G, Kaplan DL. Functionalized silk-based biomaterials for bone formation. *J Biomed Mater Res*. 2001; 54:139–148. [PubMed: 11077413]
7. Hofmann S, Hagenmüller H, Koch AM, Müller R, Vunjak-Novakovic G, Kaplan DL. Control of in vitro tissue-engineered bone-like structures using human mesenchymal stem cells and porous silk scaffolds. *Biomaterials*. 2007; 28:1152–1162. [PubMed: 17092555]
8. Park SH, Gil ES, Shai H, Kim HJ, Lee K, Kaplan DL. Relationships between degradability of silk scaffolds and osteogenesis. *Biomaterials*. 2001; 31:6162–6172. [PubMed: 20546890]
9. Cao Y, Wang B. Biodegradation of silk biomaterials. *Int J Mol Sci*. 2009; 10:1514–24. [PubMed: 19468322]
10. Cutler SM, García AJ. Engineering cell adhesive surfaces that direct integrin $\alpha 5 \beta 1$ binding using a recombinant fragment of fibronectin. *Biomaterials*. 2003; 24:1759–1770. [PubMed: 12593958]
11. Ortega N, Behonick DJ, Werb Z. Matrix remodeling during endochondral ossification. *Trends Cell Biol*. 2004; 14:86–93. [PubMed: 15102440]
12. Hayami T, Kapila YL, Kapila S. MMP-1 (collagenase-1) and MMP-13 (collagenase-3) differentially regulate markers of osteoblastic differentiation in osteogenic cells. *Matrix Biology*. 2008; 27:682–692. [PubMed: 18755271]
13. Kim HJ, Kim U, Vunjak-Novakovic G, Min B, Kaplan DL. Influence of macroporous protein scaffolds on bone tissue engineering from bone marrow stem cells. *Biomaterials*. 2005; 26:4442–4452. [PubMed: 15701373]
14. Bode W, Fernandez-Catalan C, Nagase H, Maskos K. Endoproteinase-protein inhibitor interactions. *APMIS*. 1999; 107:3–10. [PubMed: 10190274]
15. Page-McCaw A, Ewald AJ, Werb Z. Matrix metalloproteinases and the regulation of tissue remodelling. *Nat Rev Mol Cell Biol*. 2007; 8:221–233. [PubMed: 17318226]
16. Inoue K, Mikuni-Takagaki Y, Oikawa K, Itoh T, Inada M, Noguchi T, Park JS, Onodera T, Krane SM, Noda M, Itoharu S. A Crucial Role for Matrix Metalloproteinase 2 in Osteocytic Canalicular Formation and Bone Metabolism. *J Biol Chem*. 2006; 281:33814–33824. [PubMed: 16959767]
17. Mizuno M, Fujisawa R, Kuboki Y. Type I collagen-induced osteoblastic differentiation of bone-marrow cells mediated by collagen- $\alpha 2 \beta 1$ integrin interaction. *J Cell Physiol*. 2000; 184:207–213. [PubMed: 10867645]
18. Wang Y, Tan X, Zhang K. Correlation of Plasma MMP-1 and TIMP-1 Levels and the Colonic Mucosa Expressions in Patients with Ulcerative Colitis. *Mediators of Inflammation* [online]. 2009; 2009:5. Article ID 275072. 10.1155/2009/275072
19. Meikle MC, Bord S, Hembry RM, Compston J, Croucher PI, Reynolds JJ. Human osteoblasts in culture synthesize collagenase and other matrix metalloproteinases in response to osteotropic hormones and cytokines. *Journal of Cell Science*. 1992; 103:1093–1099. [PubMed: 1336777]
20. Kang CD, Lee BK, Kim KW, Kim CM, Kim SH, Chung BS. Signaling Mechanism of PMA-Induced Differentiation of K562 Cells. *Biochem Biophys Res Commun*. 1996; 221:95–100. [PubMed: 8660351]
21. Nicolin V, Baldini G, Bareggi R, Zweyer M, Zauli G, Vaccarezza M, Narducci P. Morphological features of osteoclasts derived from a co-culture system. *Journal of Molecular Histology*. 2006; 37:171–177. [PubMed: 16977429]
22. Lawrence BD, Marchant JK, Pindrus MA, Omenetto FG, Kaplan DL. Silk film biomaterials for cornea tissue engineering. *Biomaterials*. 2009; 30:1299–1308. [PubMed: 19059642]
23. Altman GH, Lu HH, Horan RL, Calabro T, Ryder D, Kaplan DL. Advanced Bioreactor with Controlled Application of Multi-Dimensional Strain For Tissue Engineering. *J Biomech Eng*. 2002; 124:742–749. [PubMed: 12596643]

24. Numata K, Kikkawa Y, Tsuge T, Iwata T, Doi Y, Abe H. Adsorption of Biopolyester Depolymerase on Silicon Wafer and Poly[(R)-3-hydroxybutyric acid] Single Crystal Revealed by Real-Time AFM. *Macromolecular Bioscience*. 2006; 6:41–50. [PubMed: 16374769]
25. Jones GL, Motta A, Marshall MJ, El Haj AJ, Cartmell SH. Osteoblast: Osteoclast co-cultures on silk fibroin.; chitosan and PLLA films. *Biomaterials*. 2009; 30:5376–5384. [PubMed: 19647869]
26. Srivastava AK, Vliet EL, Lewiecki M, Maricic M, Abdelmalek A, Gluck O, Baylink DJ. Clinical Use of Serum and Urine Bone Markers in the Management of Osteoporosis. *Curr Med Res Opin*. 2005; 21:1015–1026. [PubMed: 16004668]
27. Phillips JA, Bonassar LJ. Matrix metalloproteinase activity synergizes with $\alpha 2\beta 1$ integrins to enhance collagen remodeling. *Exp Cell Res*. 2005; 310:79–87. [PubMed: 16098964]
28. Lozito TP, Tuan RS. Mesenchymal stem cells inhibit both endogenous and exogenous MMPs via secreted TIMPs. *J Cell Physiol* [online]. 2010 epub ahead of print. 10.1002/jcp.22344
29. Knight CG, Morton LF, Onley DJ, Peachey AR, Messent AJ, Smethurst PA, Tuckwell DS, Fardale RW, Barnes MJ. Identification in Collagen Type I of an Integrin $\alpha 2\beta 1$ -binding Site Containing an Essential GER Sequence. *J Biol Chem*. 1998; 273:33287–33294. [PubMed: 9837901]
30. Zhou C, Confalonieri F, Jacquet M, Perasso R, Li Z, Janin J. Silk fibroin: Structural implications of a remarkable amino acid sequence. *Proteins: Structure ; Function; and Bioinformatics*. 2001; 44:119–122.
31. Cao Z, Huang K, Horwitz AF. Identification of a Domain on the Integrin $\alpha 5$ Subunit Implicated in Cell Spreading and Signaling. *J Biol Chem*. 1998; 273:31670–31679. [PubMed: 9822628]
32. Aota S, Nagai TS, Yamadas KM. Characterization of Regions of Fibronectin Besides the Arginine-Glycine-Aspartic Acid Sequence Required for Adhesive Function of the Cell-binding Domain Using Site-directed Mutagenesis. *J Biol Chem*. 1991; 266:15938–15943. [PubMed: 1874740]
33. Murphy AR, John PS, Kaplan DL. Modification of silk fibroin using diazonium coupling chemistry and the effects on hMSC proliferation and differentiation. *Biomaterials*. 2008; 29:2829–2838. [PubMed: 18417206]
34. Seifter, S.; Harper, E. *The enzymes*. Vol. 3. Academic Press; New York: 1971. p. 649
35. Woessner, JF.; Nagase, H. *Matrix Metalloproteinases and TIMPs*. 1. Oxford: New York; 2000. p. 101
36. Holmbeck K, Bianco P, Caterina J, Yamada S, Kromer M, Kuznetsov SA, Mankani M, Robey PG, Poole AR, Pidoux I, Ward JM, Birkedal-Hansen H. MT1-MMP-Deficient Mice Develop Dwarfism, Osteopenia, Arthritis, and Connective Tissue Disease due to Inadequate Collagen Turnover. *Cell*. 1999; 99:81–92. [PubMed: 10520996]
37. Fornaro M, Manes T, Languino LR. Integrins and Prostate Cancer Metastases. *Cancer Metastasis Rev*. 2001; 20:321–331. [PubMed: 12085969]
38. Moreau JE, Anderson K, Mauney JR, Nguyen T, Kaplan DL, Rosenblatt M. Tissue-Engineered Bone Serves as a Target for Metastasis of Human Breast Cancer in a Mouse Model. *Cancer Research*. 2007; 67:10304–10308. [PubMed: 17974972]
39. Subramanian, B.; Rudym, D.; Cannizzaro, C.; Perrone, R.; Zhou, J.; Kaplan, DL. Tissue-Engineered Three-Dimensional In Vitro Models for Normal and Diseased Kidney [published online ahead of print June 14 2010]. *Tissue Engineering Part A*. 2010. <http://dx.doi.org/10.1089/ten.tea.2009.0595>
40. Keselowsky BG, Collard DM, García AJ. Integrin binding specificity regulates biomaterial surface chemistry effects on cell differentiation. *Proceedings of the National Academy of Sciences of the United States of America*. 2005; 102:5953–5957. [PubMed: 15827122]
41. Shimo T, Matsumura S, Ibaragi S, Isowa S, Kishimoto K, Mese H, Nishiyama A, Sasaki A. Specific inhibitor of MEK-mediated cross-talk between ERK and p38 MAPK during differentiation of human osteosarcoma cells. *Journal of Cell Communication and Signaling*. 2007; 1:103–111. [PubMed: 18481201]
42. Salinas CN, Anseth KS. The enhancement of chondrogenic differentiation of human mesenchymal stem cells by enzymatically regulated RGD functionalities. *Biomaterials*. 2008; 29:2370–2377. [PubMed: 18295878]

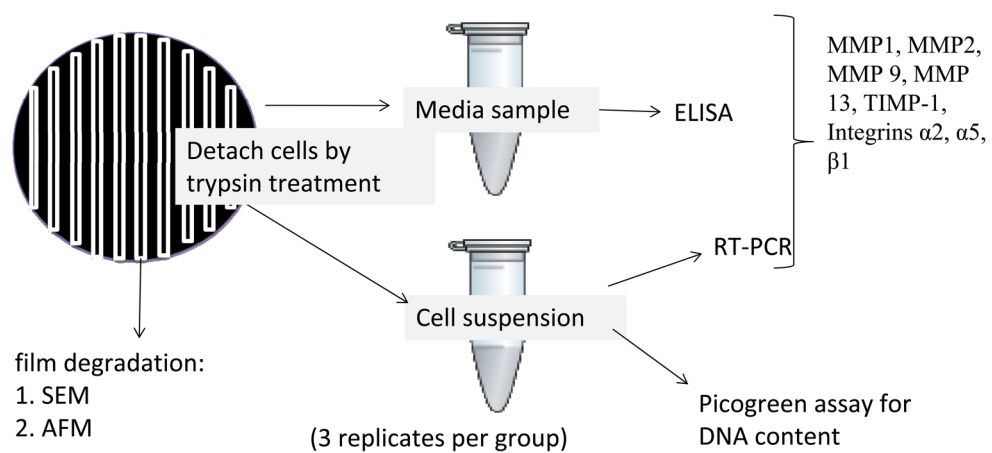


Figure 1. Schematic representation of the overall experimental procedure.

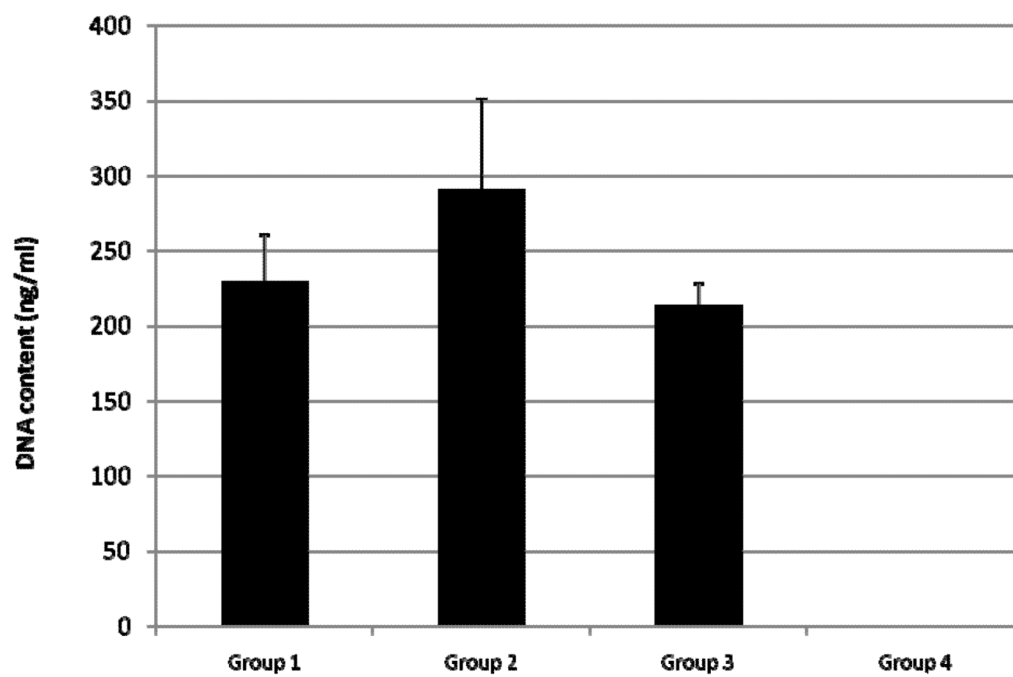


Figure 2.
DNA content of cells cultured on silk films at week 4.

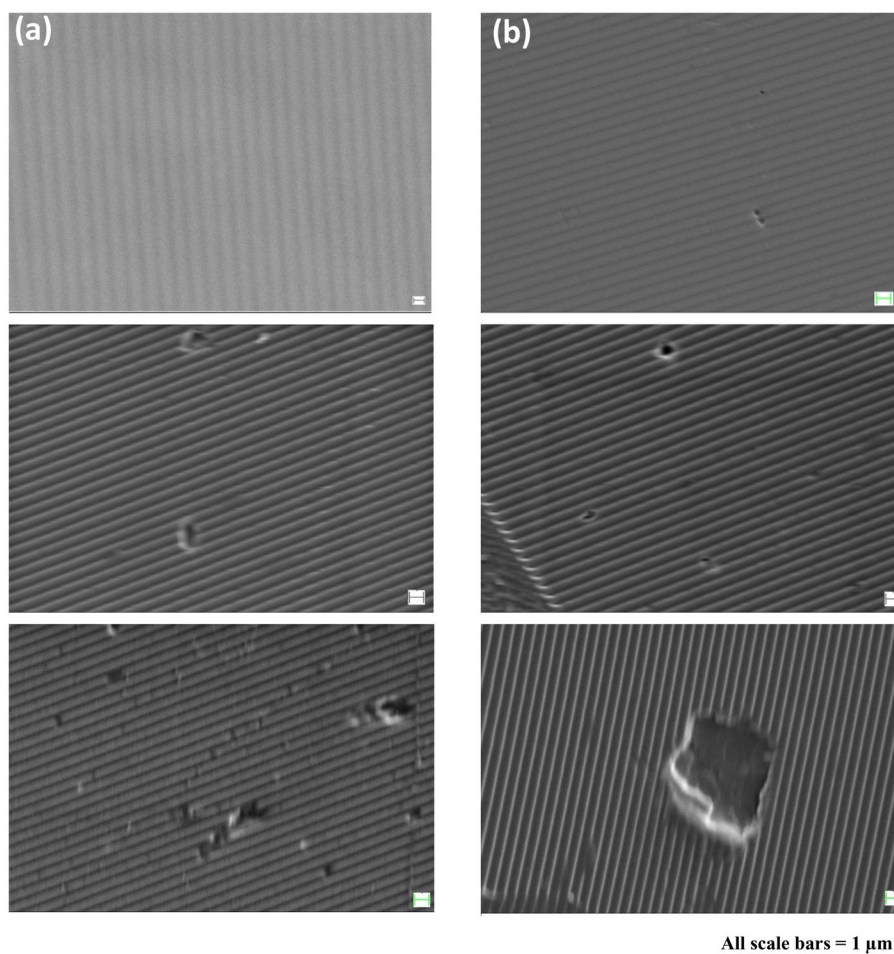
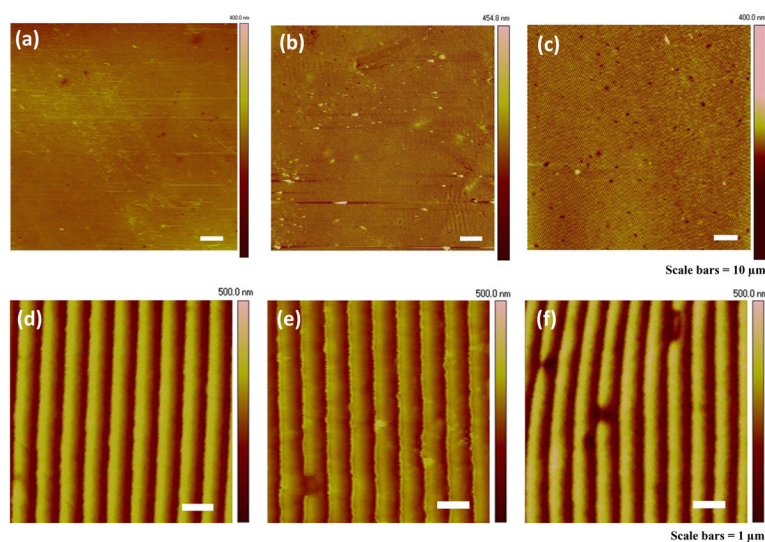


Figure 3. SEM images of degradation pits on patterned silk films caused by (a) negative control (group 4), (b) hMSCs (group 2), (c–d) osteoblasts (group 3) and (e–f) osteoclasts (group 3). All scale bars = 1 μm .

**Figure 4.**

Figures 5a–5c represent

AFM images of degradation pits on patterned silk films caused by (a) negative controls (group 4), (a) osteoblasts (group 2) and (c) osteoclasts (group 3) at scan size 100 μm . Scale bars = 10 μm . Figures 5d–5f represent AFM images of degradation pits caused by (a) negative control (group 4), (b) osteoblasts (group 2) and (c) osteoclasts (group 3) at scan size 10 μm . Scale bars = 1 μm .

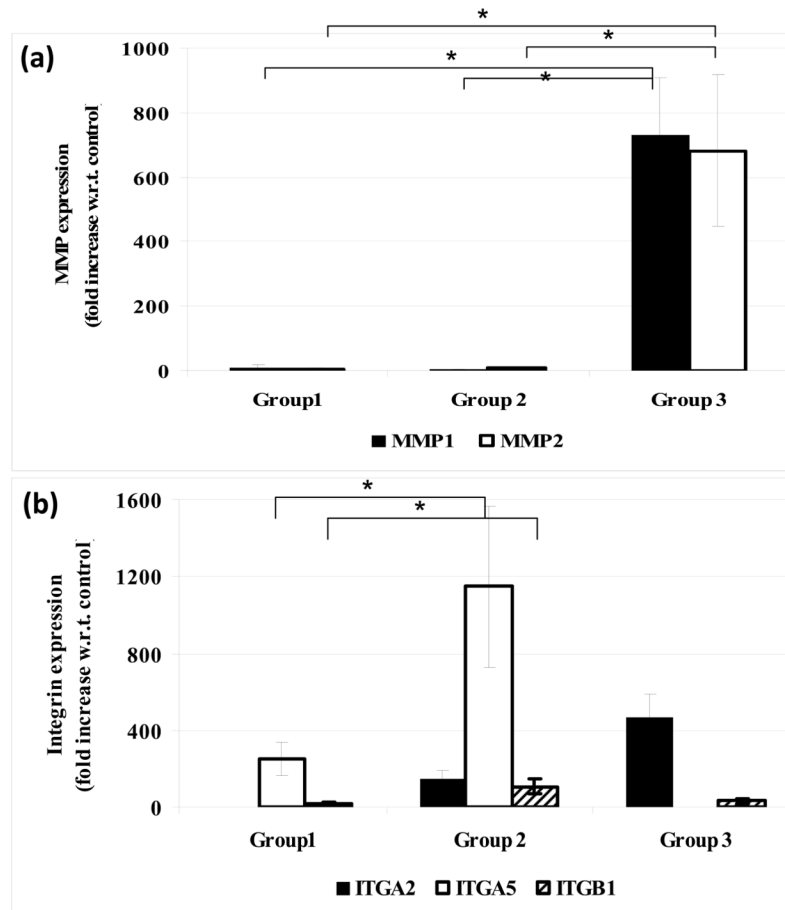


Figure 5. Transcript levels of (a) MMPs and (b) integrins in hMSCs (group 1), osteoblasts (group 2) and osteoclasts (group 3). The transcript level of each gene was normalized to the transcript level of GAPDH. Statistical significance was assigned as 8 denoting $p < 0.05$.

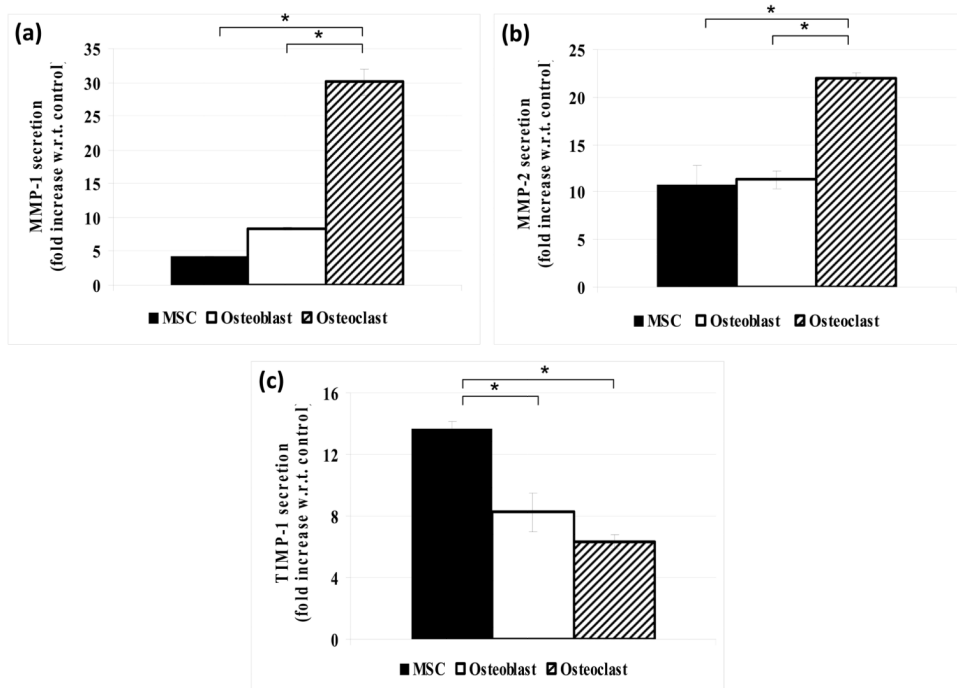


Figure 6.

(a) MMP1, (b) MMP2 and (c) TIMP-1 secretion into the media by hMSCs (group 1), osteoblasts (group 2) and osteoclasts (group 3). The protein levels secreted by each cell type were normalized to that of the negative control (group 4). Statistical significance was assigned as * denoting $p < 0.05$.

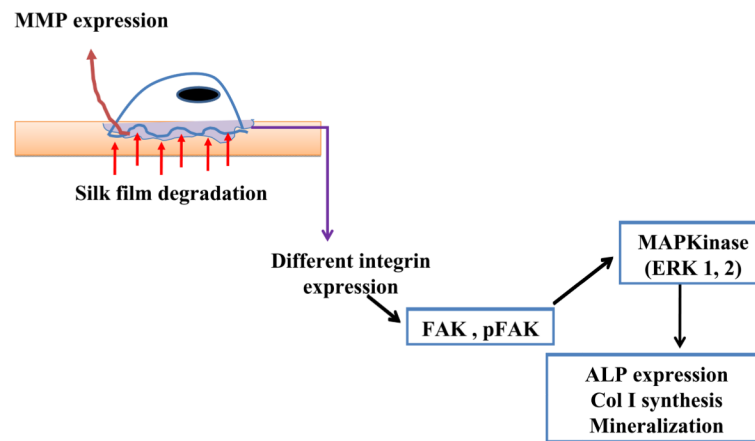


Figure 7. Schematic of possible cell signaling mechanisms triggered by MMPs and integrins to promote osteogenic differentiation on the silk film surface.

Table 1

Different groups that were assessed for their ability to degrade patterned silk films.

<i>Groups</i>	<i>Cells</i>	<i>Media</i>
1	hMSC from bone marrow	hMSC growth media
2	hMSC from bone marrow	Osteoblastic differentiation media
3	Macrophages differentiated from human THP1 Monocytes	Osteoclastic differentiation media
4	None (Negative control)	DMEM + Serum

Table 2

Comparison of degradation pits caused by osteoblasts and osteoclasts.

Cell type/Group (n=10 pits per group)	Osteoblasts (group 2)	Osteoclasts (group 3)	
<i>SEM measurement</i>			p value
Length (μm)	3.31 \pm 0.52	6.16 \pm 0.86	p<0.001
Width (μm)	2.29 \pm 0.31	3.32 \pm 0.37	p<0.01
<i>Number of pits</i>	4\pm0.93	8\pm2.26	p=0.05
<i>AFM measurement</i>			p value
Depth (nm)	53.8 \pm 6.8	72.6 \pm 11.9	p<0.05
Width (μm)	1.3 \pm 0.2	2.3 \pm 0.2	p<0.001